Estimation of Regional Evapotranspiration through Remote Sensing

FUQIN LI AND T. J. LYONS

Environmental Science, Murdoch University, Murdoch, Western Australia, Australia

(Manuscript received 9 July 1998, in final form 7 December 1998)

ABSTRACT

Models used for the remote estimation of evapotranspiration are evaluated using aircraft observations over two distinct vegetation regimes in southwestern Australia. Single-source models using an empirically determined excess resistance term performed better than a two-source model, which does not require such a parameterization. The mean absolute difference between measured and estimated values of the sensible heat flux is below 17 W m^{-2} in comparison with approximately 40 W m^{-2} for evapotranspiration. Estimates of evapotranspiration depend on the closure of the surface energy balance and incorporate all residual errors in this closure. All models performed better over the agricultural vegetation than over the native vegetation.

1. Introduction

Evapotranspiration (ET) plays a significant role in regional and global climate through the hydrological cycle, and its estimation has important applications in agriculture—in areas such as runoff prediction, recharge, crop yield prediction, land use planning, etc. (Kustas and Norman 1996; Kalma and Calder 1994). Thus, how to monitor ET efficiently has become an interdisciplinary research topic. Most conventional techniques that use point measurements to estimate ET are representative only of local areas and cannot be extended to large areas because of the dynamic nature and regional variation of ET. Remote sensing has proven to be the only suitable approach for large-area estimates of ET because satellite remote sensing is the only technology that can provide representative parameters such as radiometric surface temperature, albedo, and vegetation index in a globally consistent and economically feasible manner (Choudhury 1989; Kustas and Norman 1996).

A variety of methods and models have been developed that use remote sensing techniques to estimate ET. Physically based analytical approaches based on the Penman–Monteith resistance model and surface energy balance equations are the most common methods. They either use radiometric surface temperature to calculate the sensible heat flux H then use the energy balance equation to obtain ET, or they use radiometric surface temperature to calculate the so-called crop water stress index, then get ET. However, using radiometric surface temperature as a substitute for the aerodynamic temperature in the original Penman–Monteith model leads to substantial error, especially over partial vegetation cover, because the radiometric surface temperature is the composite temperature of soil and vegetation. This error can be reduced by introducing an extra resistance (Kustas et al. 1989, 1996), changing from single-resistance models to a two-source model, using more complicated multilayer models (Choudhury and Monteith 1988; Lhomme et al. 1994a,b; Norman et al. 1995), or developing an empirical formula to estimate the aerodynamic temperature (Huang et al. 1993), and by incorporating a vegetation index within the model (Moran et al. 1994, 1996).

The primary purpose of this paper is to evaluate models that predict ET using satellite and routine meteorological data. Three different models that are widely used are tested against aircraft observations over the Lake King area of Western Australia over both agricultural and native vegetation. Model performance is evaluated over the two different landscapes.

2. Model descriptions

a. Model 1: kB^{-1} extra-resistance model (Kustas et al. 1989)

In the extra-resistance model, H can be expressed as

$$H = \rho C_p \frac{(T_r - T_a)}{r_{ah} + r_x}, \tag{1}$$

where ρ is the air density, C_p is the specific heat of air at constant pressure, r_{ah} is the resistance to heat transfer, T_r is the radiometric surface temperature, T_a is the air

Corresponding author address: Dr. T. J. Lyons, Environmental Science, Murdoch University, Murdoch, WA 6150, Australia.
E-mail: lyons@murdoch.edu.au

temperature at reference height, and r_x is the extra resistance. The resistances are defined as

$$r_{ah} = \frac{1}{k^2 u}\left[\ln\left(\frac{z - d_0}{z_{0m}}\right) - \Psi_m\right]\left[\ln\left(\frac{z - d_0}{z_{0m}}\right) - \Psi_h\right] \quad (2)$$

and

$$r_x = \mathrm{kB}^{-1}\frac{1}{k^2 u}\left[\ln\left(\frac{z - d_0}{z_{0m}}\right) - \Psi_m\right], \quad (3)$$

where d_0 and z_{0m} are the displacement height and roughness length for momentum, k is von Kármán's constant, u is the wind speed at height z, and Ψ_h and Ψ_m are stability corrections for heat and momentum, respectively (Businger 1973; Beljaars and Holtslag 1991).

Carlson et al. (1995) noted that the parameter kB^{-1} takes into account a combination of effects: the difference between aerodynamic and radiometric temperatures, the vertical distribution of thermal radiation within the vegetation, the angular effect of radiometric temperature, energy exchanges between different surfaces, etc. Strictly speaking, this definition of kB^{-1} is a radiometric one, in contrast to the original aerodynamic definition of kB^{-1} wherein the sensible heat flux was defined in terms of the temperature difference between the surface and the atmosphere (Troufleau et al. 1997). The aerodynamic kB^{-1} is identical to $\ln(z_{0m}/z_{0h})$, where z_{0h} is the roughness length for heat. Kustas et al. (1989) found that the radiometric kB^{-1} could be expressed empirically as

$$\mathrm{kB}^{-1} = S_{\mathrm{kb}} u(T_r - T_a), \quad (4)$$

where S_{kb} is a constant between 0.05 and 0.25. The original value used by Kustas et al. (1989) was 0.17 based on their field data, but Kustas et al. (1996) later suggested that S_{kb} may be lower, at about 0.13. The average value of 0.15 has been adopted as a reference value.

The ET is calculated as the residual in the surface energy balance equation,

$$\mathrm{ET} = R_n - H - G, \quad (5)$$

where R_n is the net radiation and G is the soil heat flux.

The accuracy of this model for estimating ET is dependent not only on the estimate of H but also on the method used for estimating R_n and G, and all residual errors are incorporated in the estimate of ET.

Usually, net radiation can be estimated by

$$R_n = (1 - \alpha_t)R_s + \epsilon\sigma(\epsilon_a T_a^4 - T_r^4), \quad (6)$$

where R_s is the incoming shortwave solar radiation, α_t is the surface shortwave albedo, ϵ is the surface emissivity, σ is the Stefan–Boltzmann constant, and ϵ_a is the effective atmospheric emissivity, and with (Brutsaert 1975)

$$\epsilon_a = 1.24\left(\frac{e_a}{T_a}\right)^{1/7}, \quad (7)$$

where e_a is the atmospheric vapor pressure. The surface emissivity is calculated as a weighted average between bare soil and vegetation, such that

$$\epsilon = \epsilon_v V_c + \epsilon_s(1 - V_c), \quad (8)$$

where ϵ_v is the emissivity of vegetation (assumed to be 0.95), ϵ_s is the emissivity of bare soil (assumed to be 0.85), and V_c is the fractional vegetation cover.

Several studies have shown that G/R_n is a function of the amount of vegetation cover or the leaf area index (LAI) (Choudhury 1989). Kustas et al. (1993) indicated that a relationship existed between vegetation indices and G/R_n. Therefore, the soil heat flux can be estimated empirically using the net radiation and LAI or a satellite-derived vegetation index such as the normalized difference vegetation index (NDVI). For instance, Kustas and Daughtry (1990) proposed a linear formula and Moran et al. (1989) proposed an exponential function. Here, the Moran et al. (1989) model has been adopted as

$$G = R_n[0.58 \exp(-2.13\mathrm{NDVI})], \quad (9)$$

where NDVI = (NIR − RED)/(NIR + RED), and NIR and RED are the near-infrared and red reflectances, respectively.

b. Model 2: Soil-adjusted vegetation index model (Moran et al. 1994, 1996)

Moran et al. (1994, 1996) derived a vegetation index–temperature (VIT) trapezoid, which combines satellite vegetation indices with radiometric surface temperature, and extended crop water stress index theory (Jackson et al. 1981) to partial vegetation cover. The method is based on the hypothesis that a trapezoid shape comes from a plot of the difference between radiometric surface temperature and air temperature ($T_r - T_a$) against vegetation cover. The method assumes (Moran et al. 1994) that

1) the difference $T_r - T_a$ is a linear function of V_c and the temperature differences $T_c - T_a$ and $T_s - T_a$, such that

$$T_r - T_a = V_c(T_c - T_a) + (1 - V_c)(T_s - T_a), \quad (10)$$

where T_c is the crop foliage temperature and T_s is the soil surface temperature; and

2) for a given R_n, vapor pressure deficit of air (VPD), and aerodynamic resistance, the temperature differences $T_c - T_a$ and $T_s - T_a$ are linearly related with evaporation E and transpiration T such that

$$T_c - T_a = a + bT \quad \text{and} \quad (11)$$

$$T_s - T_a = a_{11} + b_{11}E, \quad (12)$$

where a, b, a_{11}, and b_{11} are semiempirical coefficients.

From the above assumptions, Moran et al. obtained the water deficit index (WDI), which can be expressed as

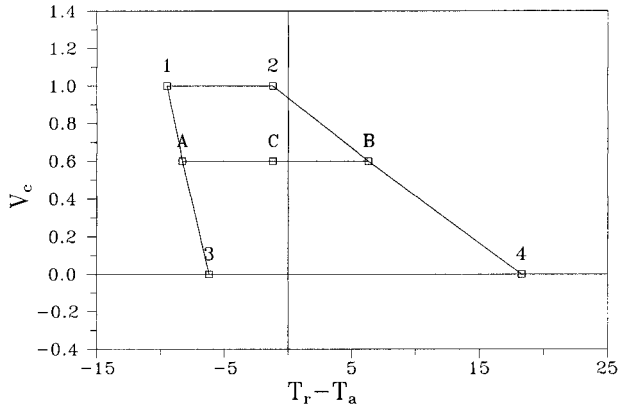

FIG. 1. Soil-adjusted vegetation index model (after Moran et al. 1994, 1996). The ''1'' represents well-watered vegetation, ''2'' = water-stressed vegetation, ''3'' = saturated bare soil, ''4'' = dry bare soil, ''A'' = well-watered with partial vegetation cover, ''B'' = water-stressed with partial vegetation cover, and ''C'' represents the actual situation.

$$\mathrm{WDI} = 1 - \frac{\mathrm{ET}}{\mathrm{ET}_p} = \left[\frac{(T_r - T_a)_m - (T_r - T_a)_r}{(T_r - T_a)_m - (T_r - T_a)_x}\right], \quad (13)$$

where ET is the surface evapotranspiration; ET_p is the potential evapotranspiration; and the subscripts m, x, and r in this case refer to the minimum, maximum, and measured values, respectively. Estimation of the maximum and minimum values is discussed by Moran et al. (1994), and Fig. 1 illustrates the model graphics, wherein WDI is equal to the ratio of the distances AC/AB.

Then,

$$\mathrm{ET} = \mathrm{ET}_p(1 - \mathrm{WDI}), \quad (14)$$

with

$$\mathrm{ET}_p = \frac{[\Delta(R_n - G) + \rho C_p \mathrm{VPD}/(r_{ah} + r_x)]}{\{\Delta + \gamma[1 + r_{cp}/(r_{ah} + r_x)]\}}, \quad (15)$$

where Δ is the slope of the saturated vapor pressure–temperature relation, γ is the psychrometric constant, and r_{cp} is the canopy resistance at potential evapotranspiration.

Moran et al. (1994) suggested that the VIT trapezoid would be more useful in remote sensing applications if V_c in Fig. 1 is substituted for by a special vegetation index that is linearly related to V_c. They suggested that the soil-adjusted vegetation index (SAVI) proposed by Huete (1988) is appropriate because SAVI is sensitive to increases in vegetation cover and insensitive to spectral changes in soil background as compared with other vegetation indices. SAVI can be expressed as

$$\mathrm{SAVI} = \frac{(\mathrm{NIR} - \mathrm{RED})}{(\mathrm{NIR} + \mathrm{RED} + L)}(1 + L), \quad (16)$$

where L is a dimensionless constant assumed to be 0.5 for a wide variety of LAI values (Huete 1988).

c. Model 3: Two-source resistance model (Lhomme et al. 1994a,b)

Lhomme et al. (1994a,b) simplified a complicated two-source model by using field data so that the two-source resistance model could be used conveniently with remotely sensed data. They obtained

$$H = \rho C_p \frac{[(T_r - T_a) - c\delta T]}{(r_{ah} + r_e)}, \quad (17)$$

where

$$\delta T = T_s - T_c, \quad (18)$$

$$c = \left\{\frac{1}{[1 + (r_{af}/r_{as})]}\right\} - V_c, \quad (19)$$

$$r_e = \frac{r_{af} r_{as}}{(r_{as} + r_{af})}, \quad (20)$$

r_{af} is the bulk boundary layer resistance of the foliage per unit ground area, and r_{as} is the aerodynamic resistance between the substrate and canopy source height. Here, r_{as} and r_{af} were calculated following Choudhury (1989) and Choudhury and Monteith (1988). The parameter kB^{-1} is not included in the aerodynamic resistance term because Lhomme et al. (1994a,b) assumed that the two-source model accounted for the bluff-body correction. Hence,

$$r_{as} = \frac{h_c \exp(\alpha)}{\alpha K_H}\left\{\exp\left(\frac{-\alpha z_{0s}}{h_c}\right) - \exp\left[\frac{-\alpha(d_0 + z_{0m})}{h_c}\right]\right\} \quad (21)$$

and

$$r_{af} = \frac{50\alpha}{\mathrm{LAI}[1 - \exp(-\alpha/2)]}\left(\frac{\omega}{u_h}\right)^{1/2}, \quad (22)$$

where

$$u_h = 1.5u\left[\ln\left(\frac{h_c - d_0}{z_{0m}}\right) \Big/ \ln\left(\frac{z - d_0}{z_{0m}}\right)\right], \quad (23)$$

$$K_H = \frac{1.5k^2(h_c - d_0)u}{\ln\left[\dfrac{(z - d_0)}{z_{0m}}\right]}, \quad (24)$$

$$\alpha = \frac{1}{\left(\dfrac{d_0}{h_c}\right)\ln\left(\dfrac{h_c - d_0}{z_{0m}}\right)}, \quad (25)$$

ω is the leaf width, z_{0s} is the aerodynamic roughness height for the soil surface, h_c is the crop canopy height, u_h is the wind speed at crop height, K_H is the eddy diffusivity at crop height, and here α is a damping coefficient for eddy diffusivity and wind speed within the canopy.

Since δT is very difficult to obtain, Lhomme et al. (1994a) assumed that

$$\delta T = a_2(T_r - T_a)^m \tag{26}$$

and adjusted the model parameters a_2 and m by comparison with field observations of H. They found that values of 0.1 and 2 for a_2 and m, respectively, provided the best fit. Later Lhomme et al. (1994b) found that a good linear relationship existed between δT and the temperature difference $T_r - T_a$, such that

$$\delta T = a_1 + b_1(T_r - T_a), \tag{27}$$

with values of 0.76 and 1.0 for a_1 and b_1, respectively.

At a temperature difference of approximately 10°C, these two δT calculations [(26), (27)] converge. Since our field site is in a semiarid region where these temperature differences are usually on the order of 10°C, we have adopted (26).

As with model 1, this model can estimate only H. The ET is obtained from the surface energy balance equation by eliminating R_n and G as before.

3. Data source

The models were validated against aircraft data from the Bunny Fence Experiment (buFex) conducted in the Lake King district of the Great Southern region of Western Australia (Fig. 2) (Lyons et al. 1993). This semiarid site is characterized by an abrupt boundary between the native and agricultural vegetation. The native vegetation is characteristically a woodland called a mallee, with *Eucalyptus eremophila* the most consistent species. Patches of eucalypt woodland occur on lower ground, and scrub heath and casuarina thickets are found on the residual plateau soil. The native vegetation is between 0.5 and 6 m high, with more than 75% of this vegetation between 0.5 and 2 m. The adjoining farmlands cultivate winter-growing annual species. Wheat is the major crop in the agricultural area and grows between May and November. Crops are generally less than 1 m high during the growing season, and, after harvest, stubbles of about 20 cm or bare soil are common (Lyons et al. 1993; Huang et al. 1993, 1995b).

Previous studies (Huang et al. 1995b; Lyons et al. 1996) have shown that the NDVI over the native vegetation is relatively constant throughout the year. In contrast, over the agricultural region, it undergoes a marked variation as transpiration increases from that of the bare soil conditions of summer to that of a developing wheat crop and then decreases with the drying out after anthesis. These studies also have shown that over the native vegetation the sensible heat flux dominates throughout the year, in marked contrast to the agricultural region where the latent heat flux is dominant throughout the growing season.

During buFex, infrared surface temperature (bandwidth 8–14 μm), humidity, potential temperature, and the three-dimensional wind components were measured

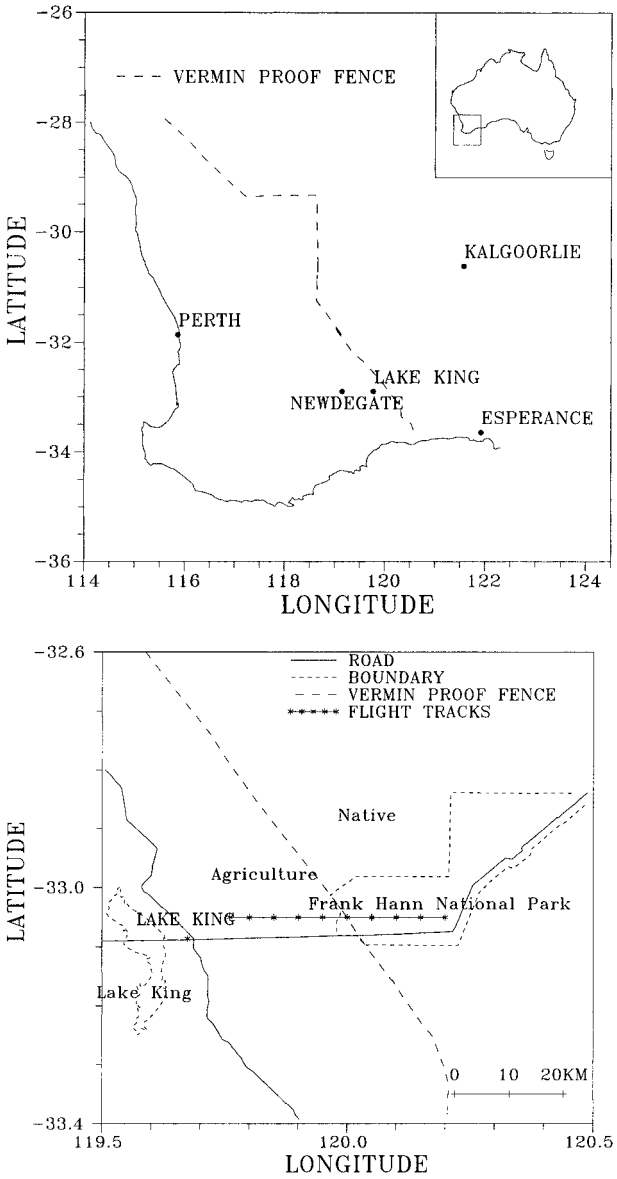

FIG. 2. Experimental site at Lake King (after Lyons et al. 1993).

by a GROB G 109B single-engine motor glider (Hacker and Schwerdtfeger 1988) at a sampling rate of 13 Hz (Lyons et al. 1993). Sensible and latent heat fluxes were evaluated by eddy correlation methods. NDVI data were obtained from the daily overpass of the National Oceanic and Atmospheric Administration satellite carrying the Advanced Very High Resolution Radiometer, using postflight calibrations for channels 1 and 2 (Smith et al. 1992).

Table 1 lists the datasets used. Preliminary aircraft data processing produced temperature, humidity, 3D wind speed, and surface temperature as a space series with an interval of 2.5 m during April and September 1992 and 2.0 m during October 1993. Aircraft measurements also provided solar radiation and albedo

TABLE 1. Date and time of experimental flights undertaken at Lake King, where WST is local standard time (UTC + 0800).

Date	Runs	Time (WST)	Runs	Time (WST)	Runs	Time (WST)
Apr 1992						
24 Apr	1–2	1317–1415	3–4	1500–1557		
25 Apr	1–2	1117–1214	3–4	1503–1603		
Sep 1992						
24 Sep	1–2	1532–1604				
25 Sep	1–2	1440–1507				
26 Sep	1–2	1138–1225	3–4	1406–1436		
28 Sep	1–2	1332–1407				
29 Sep	1–2	1032–1118	3–4	1218–1248	5–10	1419–1723
30 Sep	1–2	1200–1230	3–4	1519–1548		
Oct 1993						
4 Oct	1–2	0956–1043	3–4	1225–1312	5–8	1508–1644
5 Oct	1–2	0951–1040	3–4	1223–1313	5–6	1510–1531
6 Oct	1–2	1214–1302	3–4	1517–1606		

along the flight path, shown in Fig. 2, at altitudes between 10 and 200 m.

In analyzing the aircraft data, an 8-km cutoff wavelength was used and all aircraft observations were averaged over 20 km for both native and agricultural vegetation based on the analysis of Huang (1994). Hence, this aircraft dataset not only simulates satellite data, but provides measurements of the surface fluxes for model evaluation. Naturally, the T_r observations are essentially linear transects whereas the eddy flux data are representative of an upwind footprint, and thus there is a much larger area associated with these latter measurements. Nevertheless, the buFex site is very homogeneous on either side of the abrupt boundary.

Following Huang et al. (1995a), fractional vegetation cover in both areas was estimated from

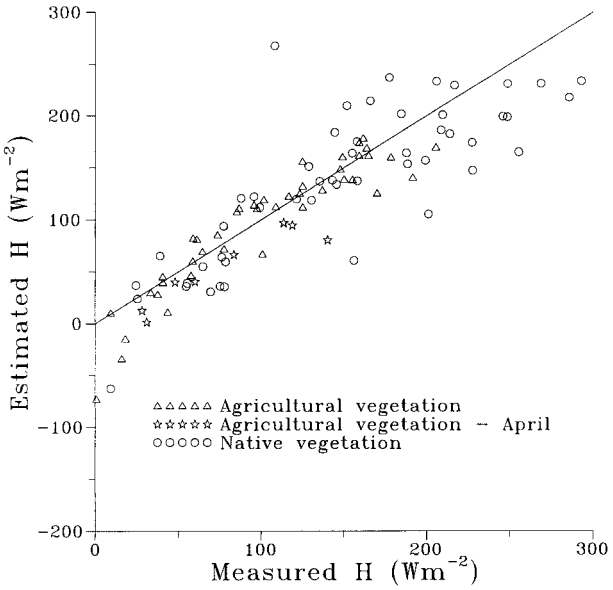

FIG. 3. Comparison of measured and model 1–estimated *H*.

$$V_c = \frac{\mathrm{NDVI}_g - \mathrm{NDVI}_{so}}{\mathrm{NDVI}_{vg} - \mathrm{NDVI}_{so}}, \tag{28}$$

where NDVI_g is the surface value of the NDVI obtained from the satellite by incorporating an atmospheric correction following Paltridge and Mitchell (1990) and by assuming aerosol optical depths of 0.1 for channel 1 and 0.07 for channel 2, respectively (Huang et al. 1995a). NDVI_{so} and NDVI_{vg} are representative values of the NDVI for bare soil and dense vegetation, respectively, obtained from direct surface observations (Huang et al. 1995a; Smith et al. 1992).

4. Results and discussion

Figure 3 shows *H* as estimated by model 1 over both agricultural and native vegetation. In the agricultural area, the model performed fairly well, with the scatter mainly falling around the 1:1 line. Over the native vegetation, the results illustrate much more scatter. The ET estimation (Fig. 4) shows different results. Over the agricultural area, ET estimation is slightly better than it is over the native vegetation although it is not as good as the *H* estimation. Since ET is the residual of the surface energy balance, these results depend on the closure of that balance.

Figure 5 and Table 2 show the aircraft-measured (H + ET) against the estimated (H + ET) expressed as ($R_n - G$) based on closure of the surface energy balance model. This comparison indicates that the model is consistently underestimating the total available energy. Since the radiation penetrating to the soil surface, which generates the surface heat flux, would increase with decreasing solar zenith angle and decreasing vegetation density, Gao et al. (1998) described the ratio of soil heat flux to net radiation as a function of solar zenith angle and the vegetation density as

$$G/R_n = \mu_1(\mathrm{NIR}/\mathrm{RED})^{\mu_2} \exp(-K/\cos\theta_s), \tag{29}$$

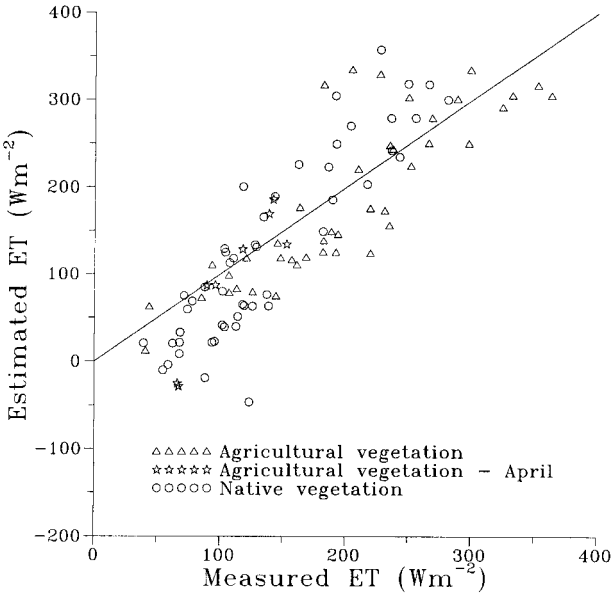

FIG. 4. Comparison of measured and model 1–estimated ET.

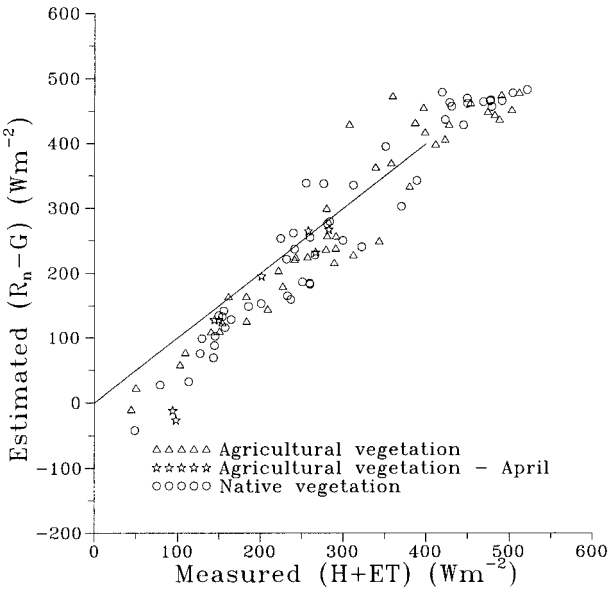

FIG. 5. Comparison of measured (H + ET) and model-estimated ($R_n - G$).

where μ_1, μ_2, and K are empirically determined numerical constants and θ_s is the solar zenith angle. Incorporation of this correction did not improve the model results, suggesting that the empirical constants have regional limitations.

In theory, model 2 would be expected to give better results as it estimates ET directly rather than via the surface energy balance. However, the fluxes from this model (Fig. 6) show that the ET estimation is not very different from model 1 over both agricultural and native vegetation.

Tables 3 and 4 illustrate how the estimated fluxes changed with S_{kb} as it ranged from its reference value of 0.15, incorporating a 10% variation up and down. In deriving these tables the following statistical parameters were defined: mean absolute difference (mad) between measured and estimated values, root-mean-square difference (rmsd) between measured and estimated values, intercept of the linear regression of measured and estimated values (a), slope of the linear regression of measured and estimated values (b), and linear correlation coefficient of measured and estimated values (r^2).

Over the agricultural vegetation, the best S_{kb} is slightly larger than 0.15. The mad and rmsd decrease with an increase of S_{kb}, whereas over the native vegetation, the results are the opposite. The smaller the S_{kb}, the better the agreement, with the best S_{kb} being smaller than 0.15. From the tables, it can be seen that the larger the S_{kb} is, the smaller is b for H. Hence, the estimated H is lower when S_{kb} is higher. With an increase in S_{kb}, the extra resistance will increase, leading to a decrease in H and an increase in estimated ET. The reason for different results between agricultural and native vegetation is related to their different surface characteristics. The S_{kb} constant theoretically depends on the roughness length, displacement height, and sensible heat flux. According to Kustas et al. (1989), kB^{-1} can be expressed as the following, based on a one-source resistance model, where H_{obs} is the measured sensible heat flux and u_* is the friction velocity:

$$kB^{-1} = \frac{ku_*(T_r - T_a)}{H_{obs}/(\rho C_p)} - \left[\ln\left(\frac{z - d_0}{z_{0m}}\right) - \Psi_h\right]. \quad (30)$$

Rearranging,

$$kB^{-1} = \frac{k^2u(T_r - T_a)}{\left(\frac{H_{obs}}{\rho C_p}\right)\left[\ln\left(\frac{z - d_0}{z_{0m}}\right) - \Psi_m\right]} - \left[\ln\left(\frac{z - d_0}{z_{0m}}\right) - \Psi_h\right], \quad (31)$$

so S_{kb} can be expressed as

TABLE 2. Statistical comparison between modeled and measured $R_n - G$.

Vegetation	$R_n - G$ median (W m^{-2})	$R_n - G$ average (W m^{-2})	mad (W m^{-2})	rmsd (W m^{-2})	a (W m^{-2})	b	r^2
Agricultural	238	261	39	50	−50	1.10	0.91
Native	252	267	39	46	−57	1.12	0.94

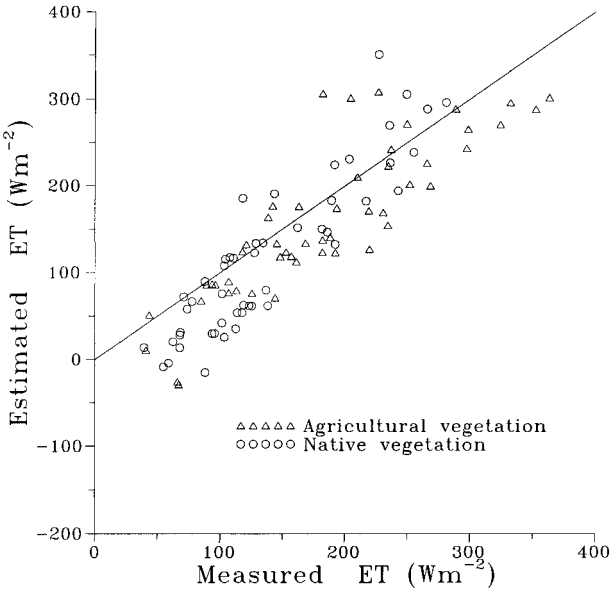

FIG. 6. Comparison of measured and model 2–estimated ET.

$$S_{\mathrm{kb}} = \frac{k^2}{\left(\frac{H_{\mathrm{obs}}}{\rho C_p}\right)\left[\ln\left(\frac{z - d_0}{z_{0m}}\right) - \Psi_m\right]} - \frac{\left[\ln\left(\frac{z - d_0}{z_{0m}}\right) - \Psi_h\right]}{u(T_r - T_a)}. \quad (32)$$

From (32), it can be seen that the surface roughness has a positive effect on S_{kb}, whereas the sensible heat flux has a negative effect. In the study area, both z_{0m} and H_{obs} are larger over the native than over the agricultural vegetation. The results shown in Tables 3 and 4 suggest that the impact of H is more significant on S_{kb} than is that of z_{0m}. Hence, S_{kb} is smaller over native vegetation than over agricultural vegetation.

Since the sensible heat flux is highly related to the temperature difference between the radiometric surface temperature and air temperature, a weak correlation between S_{kb} and the temperature difference was found in the dataset (correlation coefficient = 0.42, number of observations = 56), such that

$$S_{\mathrm{kb}} = 0.21 - 0.01(T_r - T_a). \quad (33)$$

Substituting S_{kb} values from (33) into models 1 and 2 leads to slightly better results over both areas. The rmsd decreased for both models, especially over the native vegetation (Tables 3 and 4). Model 1 had the best result over the agricultural vegetation whereas model 2 had the best result over the native vegetation.

Compared to the agricultural area, the results over the native vegetation are not as good, especially in estimating H. Choudhury (1989) suggested that for equivalent errors in estimating aerodynamic surface temperature, the resulting errors in estimating H would be larger over forests than over short vegetation, primarily because of the smaller values of aerodynamic resistance for the forest. Lyons et al. (1993) and Smith et al. (1992) also found similar results in southwestern Australia.

Since aerodynamic surface temperature is very difficult to obtain, Huang et al. (1993) developed an empirical model to estimate aerodynamic temperature and used it in a one-source resistance model to reduce the H estimation error. However, an empirical model is not uniformly applicable.

Recently, Verhoef et al. (1997) suggested that kB^{-1} over bare soil could be less than zero. However, kB^{-1} is consistently larger than zero. This result would lead to underestimating H and overestimating ET in April when the ground in the agricultural area is generally bare soil. Figure 7 shows kB^{-1} calculated from (31) compared with the results from Kustas et al.'s (1989) empirical model (4) over two different landscapes. In arriving at Fig. 7, the following criteria used by Burke and Stewart (1997) were applied: Monin–Obukhov length scale L [different from the L constant of Huete (1988)] < -1, $(T_r - T_a) > 2$ K and $u > 1.0$ m s^{-1}. When these criteria were not satisfied, data were elim-

TABLE 3. Impact of changes in S_{kb} on model results for the agricultural vegetation for sensible heat flux and evapotranspiration. Statistics are defined in the text.

	mad		rmsd		a		b		r^2	
S_{kb}	H (W m^{-2})	ET (W m^{-2})	H (W m^{-2})	ET (W m^{-2})	H (W m^{-2})	ET (W m^{-2})	H	ET	H	ET
Model 1										
0.135	19	41	24	52	−12	−15	1.10	0.98	0.86	0.72
0.15	18	40	24	51	−9	−18	1.03	1.02	0.85	0.73
0.165	18	39	25	51	−8	−21	0.96	1.06	0.84	0.74
Eq. (33)	16	38	21	47	−21	−11	1.19	0.97	0.91	0.76
Model 2										
0.135	20	45	25	55	−8	−16	1.13	0.95	0.86	0.70
0.15	18	42	23	53	−6	−19	1.05	1.00	0.85	0.72
0.165	17	41	23	53	−4	−23	0.99	1.04	0.85	0.73
Eq. (33)	18	41	22	50	−18	−12	1.22	0.93	0.92	0.74

TABLE 4. Impact of changes in S_{kb} on model results for the native vegetation.

	mad		rmsd		*a*		*b*		r^2	
S_{kb}	*H* (W m^{-2})	ET (W m^{-2})	*H* (W m^{-2})	ET (W m^{-2})	*H* (W m^{-2})	ET (W m^{-2})	*H*	ET	*H*	ET
Model 1										
0.135	34	46	46	59	15	−78	0.87	1.44	0.66	0.77
0.15	35	46	46	58	17	−77	0.81	1.49	0.66	0.79
0.165	36	47	48	58	19	−76	0.75	1.54	0.65	0.81
Eq. (33)	32	41	42	51	−6	−65	1.01	1.35	0.75	0.80
Model 2										
0.135	31	45	40	55	12	−76	0.92	1.40	0.74	0.80
0.15	31	44	40	53	14	−75	0.85	1.45	0.73	0.81
0.165	33	44	41	54	16	−74	0.79	1.50	0.72	0.82
Eq. (33)	30	39	38	48	−9	−62	1.06	1.30	0.81	0.81

inated. The average values of kB^{-1} over the agricultural and native vegetation are almost the same, at 5.16 and 5.18, respectively. These results are very different from Burke and Stewart (1997), who suggested that kB^{-1} will increase with increasing mean canopy height and with increasing z_{0m}, based on Hydrologic and Atmospheric Pilot Experiment and Sahelian Energy Balance Experiment datasets over different landscapes from a semiarid region to crops and forest. However, the diurnal variation of kB^{-1}, evident in the observations, is consistent with Verhoef et al. (1997).

Figure 8 represents *H* as estimated by model 3. It obviously overestimates *H* and the results are not as good as were achieved with models 1 and 2. These results are consistent with Zhan et al.'s (1996) analysis of the First International Satellite Land Surface Climatology Project (ISLSCP) Field Experiment (FIFE), Monsoon 90, and Washita '92 data. Model 3 also suffers from its dependence on a large number of parameters, many of which must be obtained empirically.

Tables 5 and 6 demonstrate the parameter sensitivity of the three models. The measure S_x is the sensitivity of a model to a parameter (here denoted by *x*), defined by Zhan et al. (1996) as

$$S_x = \frac{H(\mathrm{ET})_+ - H(\mathrm{ET})_-}{H_0(\mathrm{ET}_0)}, \tag{34}$$

where $H_0(\mathrm{ET}_0)$, $H(\mathrm{ET})_+$, and $H(\mathrm{ET})_-$ are the estimated sensible heat fluxes (evapotranspiration) when the parameter x_0 equals its reference value or is $1.1x_0$ and $0.9x_0$, respectively.

However, when *H* or ET values are very small, S_x is very large even if the absolute differences are very small. Therefore, another parameter A_x also is used to analyze parameter sensitivity and is defined as

$$A_x = |[H(\mathrm{ET})_+ - H(\mathrm{ET})_-]|. \tag{35}$$

The results indicate that, over both agricultural and native vegetation, the radiometric surface temperature and air temperature are very sensitive in all three models. The temperatures T_r and T_a not only directly influence *H* and ET estimation but also affect R_n and *G*, which in turn influence *H* and ET. Of the other measured

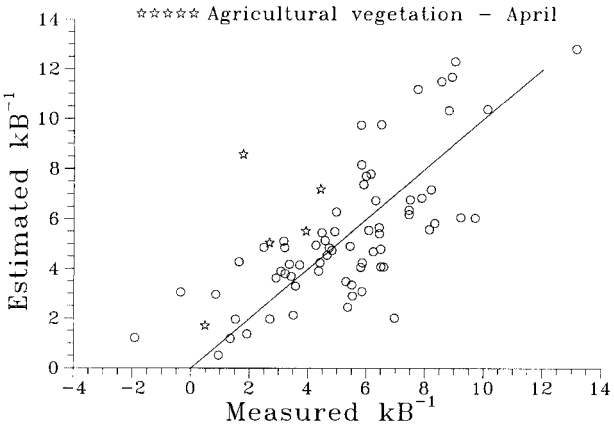

FIG. 7. Comparison of measured and estimated kB^{-1}.

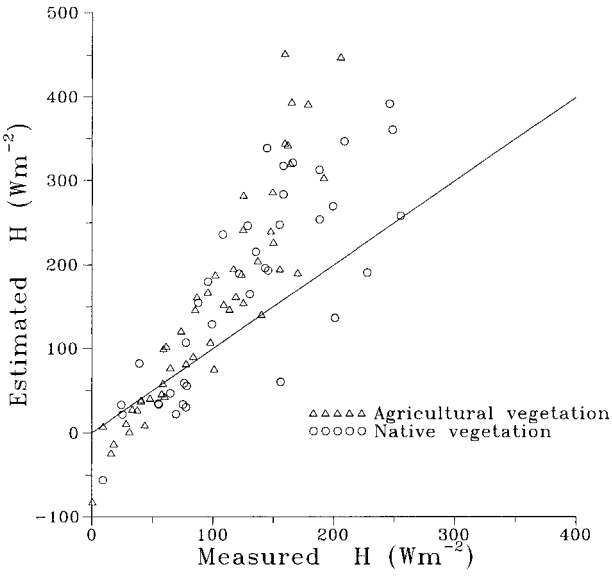

FIG. 8. Comparison of measured and model 3–estimated *H*.

TABLE 5. Average S_x and A_x values of the three models over the agricultural vegetation. Variables and statistics are defined in the text.

	Model 1				Model 2				Model 3			
	S_x		A_x		S_x		A_x		S_x		A_x	
Parameter	H	ET	H (W m^{-2})	ET (W m^{-2})	H	ET	H (W m^{-2})	ET (W m^{-2})	H	ET	H (W m^{-2})	ET (W m^{-2})
z_{0m}	0.06	0.03	6	6	0.05	0.03	5	5	0.08	1.11	18	18
S_{kb}	0.07	0.04	9	9	0.07	0.04	9	9				
u	0.12	0.06	9	9	0.10	0.06	9	9	0.19	1.32	31	31
T_r	2.28	0.94	71	88	1.85	0.97	66	84	3.00	4.80	156	173
T_a	1.85	0.80	60	70	1.57	0.81	55	61	2.83	3.30	124	134
SAVI					0.01	0.00	0	0				
$R_n - G$					0.02	0.29	1	49				
h_c									0.16	1.63	29	29
V_c									0.06	0.95	14	14
LAI									0.02	0.30	7	7
ω									0.00	0.04	0	0
a_2									0.00	0.06	1	1
m									0.02	0.31	6	6

meteorological data, wind speed is sensitive in model 3 but not in models 1 and 2.

In model 2, the difference between net radiation and soil heat flux is very sensitive to the ET estimation in both areas. However, the H estimation changed very little with $(R_n - G)$. Therefore, even though the model estimates ET directly, it still needed to estimate the net radiation and soil heat flux correctly in order to improve the ET accuracy. From this finding, it can be explained why the results of models 1 and 2 are so similar. Over both the agricultural and native vegetation, the crop parameter SAVI has little influence on the estimated ET in comparison with other parameters.

Tables 5 and 6 also indicate that in models 1 and 2 all the parameters are more sensitive to the results over the native than over the agricultural vegetation. Over the agriculture area, the results are better than over the native vegetation, since the fluxes over the native vegetation are more sensitive to parameter error.

The roughness length z_{0m} has different effects in the three models. In models 1 and 2, ET and H change little with the variation of z_{0m}, whereas model 3 is very sensitive, leading to an A_x of 29.5 W m^{-2} over the native vegetation. Crop height and vegetation cover play important roles in determining H and ET in model 3, leading to A_x values of 88 and 27 W m^{-2}, respectively, over the native vegetation. Thus, reliable estimates of these parameters are essential for improved accuracy in the application of model 3.

For the empirical parameters a_2 and m, S_x and A_x are very small in comparison with their values for other parameters, in both areas. Therefore, the figures that Lhomme et al. (1994a) obtained are suitable over a wide region.

5. Conclusions

Models 1 and 2 have similar performance over both native and agricultural vegetation, although model 2 directly calculated ET whereas model 1 arrived at it via

TABLE 6. Average S_x and A_x values of the three models over the native vegetation.

	Model 1				Model 2				Model 3			
	S_x		A_x		S_x		A_x		S_x		A_x	
Parameter	H	ET	H (W m^{-2})	ET (W m^{-2})	H	ET	H (W m^{-2})	ET (W m^{-2})	H	ET	H (W m^{-2})	ET (W m^{-2})
z_{0m}	0.08	0.19	11	11	0.07	0.19	10	10	0.09	0.58	29	29
S_{kb}	0.09	0.21	15	15	0.08	0.21	15	15				
u	0.10	0.25	12	12	0.10	0.25	12	12	0.26	1.59	75	75
T_r	1.01	2.70	81	99	0.89	2.49	74	91	1.51	7.99	236	254
T_a	0.90	2.31	67	77	0.78	2.10	61	70	1.31	6.58	183	193
SAVI					0.01	0.00	0	0				
$R_n - G$					0.01	0.65	1	54				
h_c									0.29	1.78	88	88
V_c									0.07	0.42	26	26
LAI									0.01	0.10	4	4
ω									0.01	0.16	5	5
a_2									0.00	0.04	2	2
m									0.02	0.15	11	11

closure of the surface energy balance. Both models provided better estimates than did the more sophisticated model 3.

Both models 1 and 2 depend on S_{kb}, which was found to have a weak relationship with the temperature difference between radiometric surface temperature and air temperature. Incorporating this relationship led to slightly improved results, with model 1 giving the best result over the agricultural area and model 2 giving the best result over the native vegetation.

Tables 5 and 6 highlight the limitations of these models when air temperature is not measured or if it varies much over a region. For regional-scale applications, it may be difficult to use these approaches in areas where there is a very sparse network of air temperature and wind speed observations. The application of single-source approaches over various landscapes will be tenuous because kB^{-1} as formulated in models 1 and 2 is affected not only by the aerodynamic properties of the surface but also by H itself. Furthermore, other factors that affect the T_r observation, such as the amount of bare soil/substrate viewed by the radiometer, have been shown to be uncorrelated to the flux (Sun and Mahrt 1995).

The results for model 3 are more dependent on the empirical parameters within the model. These results are consistent with the recent analysis of Zhan et al. (1996) based on FIFE, Monsoon 90, and Washita '92 data.

Acknowledgments. The buFex was a joint field experiment funded by the Australian Research Council, Murdoch University's Special Research Grant, the CSIRO–Flinders University Collaborative Grant Scheme, the Western Australian Department of Agriculture, and the Leeuwin Remote Sensing Centre. Throughout this research, Fuqin Li was in receipt of an Overseas Postgraduate Research Award and associated Murdoch University Research Scholarship. The comments of anonymous referees also benefited this work. All of this assistance is gratefully acknowledged.

REFERENCES

Beljaars, A. C. M., and A. A. M. Holtslag, 1991: Flux parameterization over land surfaces for atmospheric models. *J. Appl. Meteor.,* **30,** 327–341.

Brutsaert, W. H., 1975: On a derivable formula for long-wave radiation from clear skies. *Water Resour. Res.,* **11,** 742–744.

Burke, E. J., and J. B. Stewart, 1997: Test of a sensible heat flux–radiometric surface temperature relationship for HAPEX-Sahel. *Bound.-Layer Meteor.,* **84,** 329–337.

Businger, J. A., 1973: Turbulent transfer in the atmospheric surface layer. *Workshop on Micrometeorology,* D. A. Haugen, Ed., Amer. Meteor. Soc., 67–100.

Carlson, T. N., O. Taconet, A. Vidal, R. R. Gillies, A. Olioso, and K. Humes, 1995: An overview of the workshop on thermal remote sensing held at La Londe les Maures, France, September 20–24, 1993. *Agric. For. Meteor.,* **77,** 141–151.

Choudhury, B. J., 1989: Estimating evaporation and carbon assimilation using infrared temperature data: Vistas in modelling. *Theory and Applications of Optical Remote Sensing,* G. Asrar, Ed., John Wiley and Sons, 628–690.

——, and J. L. Monteith, 1988: A four-layer model for the heat budget of homogeneous land surfaces. *Quart. J. Roy. Meteor. Soc.,* **114,** 373–398.

Gao, W., R. L. Coulter, B. M. Lesht, J. Qiu, and M. L. Wesely, 1998: Estimating clear-sky regional surface fluxes in the southern Great Plains Atmospheric Radiation Measurement site with ground measurements and satellite observations. *J. Appl. Meteor.,* **37,** 5–22.

Hacker, J. M., and P. Schwerdtfeger, 1988: The FIAMS Research Aircraft System description. FIAMS Tech. Rep. 8, Flinders University of South Australia, 60 pp. [Available from Flinders Institute for Atmospheric and Marine Sciences, Flinders University of South Australia, GPO Box 2100, Adelaide, S.A. 5000, Australia.]

Huang, X., 1994: Land atmospheric interaction in a semi-arid region. Ph.D. thesis, Murdoch University, 212 pp. [Available from Library, Murdoch University, Murdoch, W.A. 6150, Australia.]

——, T. J. Lyons, R. C. G. Smith, J. M. Hacker, and P. Schwerdtfeger, 1993: Estimation of surface energy balance from radiant surface temperature and NOAA AVHRR sensor reflectances over agricultural and native vegetation. *J. Appl. Meteor.,* **32,** 1441–1449.

——, ——, ——, and ——, 1995a: Estimation of land surface parameters using satellite data. *Hydrol. Processes,* **9,** 631–643.

——, ——, and ——, 1995b: Meteorological impact of replacing native perennial vegetation with annual agricultural species. *Hydrol. Processes,* **9,** 645–654.

Huete, A. R., 1988: A soil-adjusted vegetation index (SAVI). *Remote Sens. Environ.,* **25,** 295–309.

Jackson, R. D., S. B. Idso, R. J. Reginato, and P. J. Pinter Jr., 1981: Canopy temperature as a crop water stress indicator. *Water Resour. Res.,* **17,** 1133–1138.

Kalma, J. D., and I. R. Calder, 1994: Land surface processes in large-scale hydrology. World Meteorological Organization Operational Hydrology Rep. 40, 60 pp.

Kustas, W. P., and C. S. T. Daughtry, 1990: Estimation of the soil heat flux/net radiation ratio from spectral data. *Agric. For. Meteor.,* **49,** 205–223.

——, and J. M. Norman, 1996: Use of remote sensing for evapotranspiration monitoring over land surfaces. *Hydrol. Sci.—J. Sci. Hydrol.,* **41,** 495–516.

——, B. J. Choudhury, M. S. Moran, R. J. Reginato, R. D. Jackson, L. W. Gay, and H. L. Weaver, 1989: Determination of sensible heat flux over sparse canopy using thermal infrared data. *Agric. For. Meteor.,* **44,** 197–216.

——, C. S. T. Daughtry, and P. J. Van Oevelen, 1993: Analytical treatment of the relationships between soil heat flux/net radiation ratio and vegetation indices. *Remote Sens. Environ.,* **46,** 319–330.

——, K. S. Humes, J. M. Norman, and M. S. Moran, 1996: Single- and dual-source modeling of surface energy fluxes with radiometric surface temperature. *J. Appl. Meteor.,* **35,** 110–121.

Lhomme, J.-P., B. Monteny, and M. Amadou, 1994a: Estimating sensible heat flux from radiometric temperature over sparse millet. *Agric. For. Meteor.,* **68,** 77–91.

——, ——, A. Chehbouni, and D. Troufleau, 1994b: Determination of sensible heat flux over Sahelian fallow savannah using infrared thermometry. *Agric. For. Meteor.,* **68,** 93–105.

Lyons, T. J., P. Schwerdtfeger, J. M. Hacker, I. J. Foster, R. C. G. Smith, and X. Huang, 1993: Land–atmosphere interaction in a semiarid region: The Bunny Fence Experiment. *Bull. Amer. Meteor. Soc.,* **74,** 1327–1334.

——, R. C. G. Smith, and X. Huang, 1996: The impact of clearing for agriculture on the surface energy budget. *Int. J. Climatol.,* **16,** 551–558.

Moran, M. S., R. D. Jackson, L. H. Raymond, L. W. Gay, and P. N. Slater, 1989: Mapping surface energy balance components by combining Landsat Thematic Mapper and ground-based meteorological data. *Remote Sens. Environ.,* **30,** 77–87.

——, T. R. Clarke, Y. Inoue, and A. Vidal, 1994: Estimating crop water deficit using the relation between surface-air temperature and spectral vegetation index. *Remote Sens. Environ.,* **49,** 246–263.

——, A. F. Rahman, J. C. Washburne, D. C. Goodrich, M. A. Weltz, and W. P. Kustas, 1996: Combining the Penman–Monteith equation with measurements of surface temperature and reflectance to estimate evaporation rates of semiarid grassland. *Agric. For. Meteor.,* **80,** 87–109.

Norman, J. M., W. P. Kustas, and K. S. Humes, 1995: A two-source approach for estimating soil and vegetation energy fluxes in observations of directional radiometric surface temperature. *Agric. For. Meteor.,* **77,** 263–293.

Paltridge, G. W., and R. M. Mitchell, 1990: Atmospheric and viewing angle correction of vegetation indices and grassland fuel moisture content derived from NOAA-AVHRR. *Remote Sens. Environ.,* **31,** 121–135.

Smith, R. C. G., X. Huang, T. J. Lyons, J. M. Hacker, and P. T. Hick, 1992: Change in land surface albedo and temperature in southwestern Australia following the replacement of native perennial vegetation by agriculture: Satellite observations. World Space Congress IAF-92-0117, International Astronautical Federation, 10 pp. [Available from International Astronautical Federation, 3-5, Rue Mario-Nikis, 75015 Paris, France.]

Sun, J., and L. Mahrt, 1995: Relationship of surface heat flux to microscale temperature variations: Applications to BOREAS. *Bound.-Layer Meteor.,* **76,** 291–301.

Troufleau, D., J.-P. Lhomme, B. Monteny, and A. Vidal, 1997: Sensible heat flux and radiometric surface temperature over sparse Sahelian vegetation. 1. An experimental analysis of the kB^{-1} parameter. *J. Hydrol.,* **188–189,** 815–838.

Verhoef, A., H. A. R. De Bruin, and B. J. J. M. Van Den Hurk, 1997: Some practical notes on the parameter kB^{-1} for sparse vegetation. *J. Appl. Meteor.,* **36,** 560–572.

Zhan, X., W. P. Kustas, and K. S. Humes, 1996: An intercomparison study on models of sensible heat flux over partial canopy surfaces with remotely sensed surface temperature. *Remote Sens. Environ.,* **58,** 242–256.